INTEGRATED INTERCEPT MISSILE GUIDANCE AND CONTROL WITH TERMINAL ANGLE CONSTRAINT

H. S. Shin*, T. W. Hwang, A. Tsourdos***, B. A. White***, M. J. Tahk***
***KAIST, Daejeon 305-701, Republic of Korea**
****Agency for Defence Development, Daejeon 305-600, Rep. of Korea**
*****Cranfield University, Shrivenham, Swindon SN6 8LA, United Kingdom**

Keywords: *Integrated guidance and control, Interception, Terminal angle constraint, Lyapunov candidate function, Backstepping, Disturbance observer*

Abstract

This paper examines the proposed integrated backstepping design of missile guidance and control to the engagement of manoeuvring targets. To control engagement geometry, impact-angle-control guidance (IAGC) is analysed in two dimensional geometry. The integrated backstepping design with disturbance observer is then developed and interpreted in view of stability and robustness. The performance of designed algorithm is verified via numerical simulation.

Nomenclature

α	Angle-of-attack (AOA)
q	Angular pitch rate
A_z	Acceleration tangent to body z-axis
δ	Actuator deflection angle for pitch control
C_{D0}	Zero-lift drag coefficient
U	Velocity along body x-axis
$\bar{Q}$	Dynamic pressure
m	Mass
I_{yy}	Inertia of body y-axis
S	Reference surface
d_{ref}	Reference code
η	Actuator deflection angular rate

1 Introduction

Over the recent past, the tendency of guidance system has been to rely more on precision and manoeuvrability with small warhead than on large missiles with a large warhead [1], [2]. Both of missile and guided weapon system have becoming more accurate and sophisticated based on development of sensor technology and control theory, but the targets have also become more intelligent and stealthy. Thus, it is required to design an aerial system which has high-angle-of-attack manoeuvrability and operation capability over a broad flight envelop, and to design better guidance algorithms that can intercept smaller and more manoeuvrable targets that are difficult to detect and track. Robustness about model errors has been primary check point for modern control design owing to high-angle-of-attack stability variation, pitch-roll-yaw coupling effects, and nonlinear aerodynamics with uncertainties cased by expanded covering range of missiles. Moreover, because of the reliance on more precision and smaller warheads, the endgame geometry has also become more important to enable aim-point selection and approach direction to be controlled. These trends require greater control of the engagement trajectory for the terminal guidance phase. Traditional Proportional Navigation does not allow for the control of the trajectory, but is not-the-less a robust solution. Hence there is a need for equally robust guidance solutions that allow for greater flexibility in the engagement trajectory.

First contribution of this paper is analysis and interpretation of proposed impact-angle-control guidance (IACG) that will ensure manoeuvring target interception and achieve the desired impact angle. The purpose of IACG is to design missile guidance law which can intercept target and control engagement geometry [9]. IACG has been widely studied and used to satisfy the flight path angle constraint for several reasons [10], [11]. For anti-ship or antitank missiles, the terminal impact angle is important for warhead effect. Especially, it is well known for missiles that vertical impact on the target can reduce the miss distance produced by navigation errors. It can also be generalized for an unmanned aerial vehicle which has flight-path constraints depending on its mission.

Second contribution is integration the proposed IACG and control law using backstepping control method. Although there are numerous methods to produce an entire system of guidance and control, it is typical and dominant to design each component separately and then integrate them for complete system [4]. However, integrated design of guidance and control has attracted considerable attention for a recent decade [3], [4], [7], [13], [12]. Integrated guidance and control methodology not only improve hitting performance but also it is powerful to design robust control law when a model has disturbances and uncertainties [3], [4].

Final Contribution of this paper is study for implementation issues and analysis for robustness of proposed algorithm. For real application, it is important how simply the algorithm is implemented and how robustly the proposed method keeps reasonable performance under big uncertainties. The algorithm should not be complicated and the sensor information should not be difficult to measure for simple and practical implementation [6]. Thus, state estimation has been another important issue for integrated guidance and control [5], [14]. In this paper, it is assumed the sensor tracking the target, either in the missile nose or as a third party sensor, will give the following information:

1) Range
2) Range rate
3) Line of sight angle
4) Line of sight angle rate

In real application of missile guidance, these parameters have been used because we can measure. Every guidance and control command is composed by simple multiplication of above information and missiles motion information. Moreover, high order sliding mode disturbance observer is considered in order to guarantee robustness. The effectiveness and applicability of the proposed integrated guidance and control logic is verified by numerical simulations. The longitudinal dynamics of the missiles and kinematics of engagement geometry are used.

2 Missile Model

Linearised missile dynamics in a pitch plane are given by:

$$\begin{aligned} \dot{\alpha} &= Z_\alpha \alpha + Z_\delta \delta + q + \Delta\alpha \\ \dot{q} &= M_\alpha \alpha + M_q q + M_\delta \delta \Delta q \\ A_z &= (Z_\alpha \alpha + Z_\delta \delta) U \end{aligned} \tag{1}$$

with:

$$\begin{aligned} Z_\alpha &= -\frac{\bar{Q}S}{m}(C_{D0} + C_{L\alpha}) \\ Z_\delta &= -\frac{\bar{Q}S}{m} C_{L\delta} \\ M_\alpha &= \frac{\bar{Q}Sd_{ref}}{I_{yy}} C_{m\alpha} \\ M_q &= \frac{\bar{Q}Sd_{ref}^2}{I_{yy}} C_{mq} \\ M_\delta &= -\frac{\bar{Q}Sd_{ref}}{I_{yy}} C_{m\delta} \end{aligned} \tag{2}$$

where C_X represents the static or dynamic aerodynamic derivatives, i.e., $C_{L\alpha}$ is the derivative of the lift coefficient w.r.t. α, and $\Delta\alpha$ and Δq are unknown aerodynamics and nonlinear dynamics term. In order to design a guidance and control law of missile, which kinds of measurements are available is important. Basically, a normal missile has accelerometers and rate gyros sensors to measure the own motion information. When it is assumed that the missile is equipped only these sensors, state equation (39) can be rewritten as:

$$\begin{aligned}\dot{A}_z &= \bar{Z}_A A_z + \bar{Z}_q q + \bar{Z}_\eta \eta + \Delta A_z \\ \dot{q} &= M_A A_z + M_q q + M_\delta \delta + \Delta q \end{aligned} \tag{3}$$

with:

$$\begin{aligned}\bar{Z}_A &= Z_\alpha, \ \ \bar{Z}_q = UZ_\alpha, \ \ \bar{Z}_\eta = UZ_\delta \\ \bar{M}_A &= \frac{M_\alpha}{UZ_\alpha}, \ \ \bar{M}_q = M_q, \ \ \bar{M}_\delta = (M_\delta - \frac{M_\delta Z_\delta}{Z_\alpha}) \end{aligned} \tag{4}$$

where ΔA_z is unknown disturbance term for the acceleration A_z dynamics. Note that the term $\bar{Z}_\eta \eta$ is related to nonminimum phase characteristics, and the actuator deflection angular rate η is difficult to be measured. Therefore, missile dynamics equation (3) can be reintroduced under assumption that the unknown disturbance ΔA_z includes the term, in the form:

$$\begin{aligned}\dot{A}_z &= \bar{Z}_A A_z + \bar{Z}_q q + \Delta A_z \\ \dot{q} &= M_A A_z + M_q q + M_\delta \delta + \Delta q \end{aligned} \tag{5}$$

3 Guidance Strategy

3.1 Homing Guidance

Consider a planar engagement scenario of two vehicles shown in Fig. 1. The two-dimensional (2-D) point mass model is used in homing guidance problem for the simplicity. In this figure, subscript M and T denote motion information of the missile and target, respectively, i.e., $\mathbf{v}_M$ and $\mathbf{v}_T$ represent velocity vector of the missile and target. And, ρ means the relative distance, λ and γ represent the line-of-sight (LOS) angle and the flight path angle, respectively. The I-frame is the inertial reference frame and all information of the motions of vehicles is described with respect to the inertia reference frame.

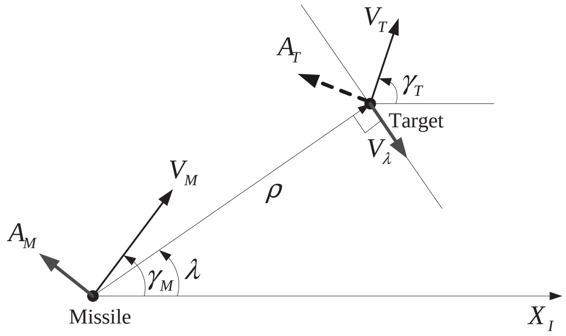

Fig. 1 Guidance geometry

From the missile guidance geometry shown in Fig. 1, the relative distance of the follower with respect to the target and LOS angle are obtained as:

$$\rho = \sqrt{\rho_X^2 + \rho_Y^2} \tag{6}$$

$$\lambda = \tan^{-1}\frac{\rho_Y}{\rho_X} \tag{7}$$

where $\rho_X = \rho\cos\lambda$ and $\rho_Y = \rho\sin\lambda$. Under assumption of constant speed of the missile and target, kinematics of missile to range and LOS angle are governed by:

$$\begin{aligned}\dot{\rho} &= \frac{\rho_X\dot{\rho}_X + \rho_Y\dot{\rho}_Y}{\rho} \\ &= V_T\cos(\gamma_T - \lambda) - V_M\cos(\gamma_M - \lambda) \\ \dot{\lambda} &= \frac{\rho_X\dot{\rho}_Y - \rho_Y\dot{\rho}_X}{\rho^2} \\ &= \frac{V_T\sin(\gamma_T - \lambda) - V_M\sin(\gamma_M - \lambda)}{\rho} \\ \dot{\gamma}_T &= \frac{A_T}{V_T} \\ \dot{\gamma}_M &= \frac{A_M}{V_M} \end{aligned} \tag{8}$$

In conventional homing guidance using proportional navigation (PN) concept, a guidance law is designed to make and maintain LOS rate $\dot{\lambda}$ as zero because it is possible to intercept a target when LOS angle is sustained as constant. Similarly, if zero effort transversal miss distance perpendicular to LOS [1] becomes zero during total homing phase, a missile can accomplish the homing mission. To design a guidance law for interception, new sliding manifold σ is introduced as equation (9) in this report.

$$\begin{aligned} \sigma &\equiv V_\lambda = \frac{ZEM_{PLOS}}{t_{go}} \\ &= \rho\dot{\lambda} \qquad (9) \\ ZEM_{PLOS} &= t_{go}\rho\dot{\lambda} \end{aligned}$$

where t_{go}, ZEM_{PLOS}, and V_λ are time-to-go, zero effort transversal miss distance, and a relative velocity normal to LOS, respectively. Note that the sliding manifold has to be zero to intercept a target. Let us consider Lyapunov candidate function in order to guarantee homing to the target:

$$V_{PROP} = \frac{1}{2}\sigma^2 \qquad (10)$$

The governing dynamic of the proposed sliding manifold derived as:

$$\begin{aligned} \dot{\sigma} &= \dot{\rho}\dot{\lambda} + \rho\ddot{\lambda} \\ &= -\dot{\rho}\dot{\lambda} + A_\lambda \qquad (11) \\ A_\lambda &= \rho\ddot{\lambda} + 2\dot{\rho}\dot{\lambda} \qquad (12) \end{aligned}$$

Thus, the time derivative of Lyapunov candidate function Eqn. 10 is derived as:

$$\begin{aligned} \dot{V}_{PROP} &= V_\lambda\dot{\sigma} \\ &= \sigma(-\dot{\rho}\dot{\lambda} + A_\lambda) \qquad (13) \end{aligned}$$

Since $\dot{V}_{PROP}$ should be negative definite with respect to σ for asymptotical stability, A_λ is taken as:

$$A_\lambda = \dot{\rho}\dot{\lambda} - K_1 V_\lambda \qquad (14)$$

Substituting of equation (14) into equation (13) yields:

$$\begin{aligned} \dot{V}_{PROP} &= -K_1 V_\lambda^2 \\ &\leq 0 \qquad (15) \end{aligned}$$

Traditional PNG acceleration command, V_{PNG}, also can be one of candidate to satisfy equation (13) as:

$$\begin{aligned} \dot{V}_{PNG} &= -(N-1)\frac{V_\lambda^2}{t_{go}} \\ &\leq 0 \qquad (16) \end{aligned}$$

Since t_{go} decreases to zero in homing phase, V_{PNG} of equation (16) in initial homing phase is much closer to zero than that of the final. If K_1 is set to $N-1$, V_{PNG} is larger than V_{PROP} until t_{go} becomes 1 second. It means that the V_λ convergence speed of the proposed guidance command is faster than the speed of PNG in initial guidance phase. Moreover, proposed acceleration command of final homing phase is within acceptable bound, while PNG generally deduce large or saturated homing acceleration command in final homing phase.

3.2 Impact Angle Control

Impact angle θ_i is defined as the angle between two velocity vectors at the interception point:

$$\theta_i = \gamma_M(t_f) - \gamma_T(t_f) \qquad (17)$$

where t_f is the impact time, i.e., the time at the interception point. Since a IACG must guarantee homing and the same impact angle with desired one simultaneously, it is necessary to define two coupled sliding surfaces for designing a IACG using the backstepping method. Whilst both the first time derivatives of equation (9) and (17) include same guidance command, it is impossible to define these two equations as sliding surfaces because they are decoupled.

In order to find a new sliding surface for a IACG, in other words homing guidance with terminal angle constraint, consider the engagement geometry of the missile and target as shown in Fig. 2. From the figure, it is obvious that the im-

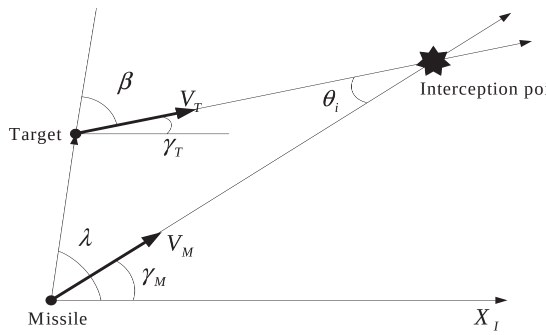

Fig. 2 Engagement geometry

pact angle can be controlled by setting the desired LOS angle. In this paper, a sliding surface corresponding to the impact angle is introduced as:

$$\sigma_1 = \lambda - \lambda_c \tag{18}$$

When there is no lateral acceleration of the target, λ_c is given by [9]:

$$\lambda_c = \gamma_T + \beta \tag{19}$$

where β is a new parameter determined by the impact angle. As shown Fig. 2, under assumption that the velocities of the missile and target are constant, applying sine rule to the geometry of the interception course provides a matching condition to find β:

$$\begin{aligned} \frac{\tau}{\sin\beta} &= \frac{1}{\sin(\beta-\theta_i)} \\ \tau &= \frac{V_M}{V_T} \end{aligned} \tag{20}$$

And, from this equation, we have:

$$\beta = \tan^{-1}\left(\frac{\tau\sin\theta_i}{\tau\cos\theta_i - 1}\right) \tag{21}$$

Hence, for IACG, two sliding surfaces are proposed as:

$$\begin{aligned} \sigma_1 &= \lambda - \lambda_c \\ \sigma_2 &= V_\lambda \end{aligned} \tag{22}$$

If there is target's lateral acceleration, the engagement geometry is different from Fig. 2 so λ_c has to be different from equation (19). This problem will be considered in our future work.

Backstepping control design is a recursive procedure, which breaks down the control problem into a sequence of lower-order control problems and determines the virtual control inputs providing the Lyapunov stability for each subproblem and overall system. In order to design the IACG which can guarantee the stability of the guidance system, a backstepping control method is considered. The main idea of backstepping is to introduce pseudo control for Lyapunov stability. In this paper, the new residual variables z_1, z_2 and virtual control states σ_{2c} is proposed as:

$$\begin{aligned} z_1 &= \sigma_1 \\ z_2 &= \sigma_2 - \sigma_{2c} \end{aligned} \tag{23}$$

The first time derivative of the residual variables are given by:

$$\begin{aligned} \dot z_1 &= \frac{z_2}{\rho} + \frac{\sigma_{2c}}{\rho} - \dot\lambda_c \\ \dot z_2 &= -\dot\rho\dot\lambda + A_\lambda - \dot\sigma_{2c} \end{aligned} \tag{24}$$

The stability of the guidance algorithm can be determined by use of a simple Lyapunov function of the form:

$$V_{IACG} = \frac{z_1^2}{2} + \frac{z_2^2}{2} \tag{25}$$

For stability, the time derivative of the function V_{IACG} has to be negative semi-definite. Thus, σ_{2c} and A_λ is proposed as:

$$\begin{aligned} \sigma_{2c} &= \rho\dot\lambda_c - K_1 z_1 \\ A_\lambda &= \dot\sigma_{2c} + \dot\rho\dot\lambda - \frac{z_1}{\rho} - K_2 z_2 \end{aligned} \tag{26}$$

where K_1, K_2 are positive. Substituting this equation into the time derivative $\dot V_{IACG}$ yields:

$$\begin{aligned} \dot V_{IACG} &= -K_1 z_1^2 - K_2 z_2^2 \\ &\leq 0 \end{aligned} \tag{27}$$

This equation represents the proposed IACG system is stable.

4 Integrated Guidance and Control Law

4.1 Backstepping Control Design

In order to design the integrated missile interception guidance and control , the backstepping control method is also considered in this section. It is necessary to redefine plant dynamics for integrated backstepping design of missile guidance and control. For the new dynamics of backstepping design, the first time derivatives of the sliding surfaces are reintroduced:

$$\begin{aligned} \dot\sigma_1 &= \dot\lambda - \Delta\sigma_1 \\ \dot\sigma_2 &= -\dot\rho\dot\lambda + A_z + \Delta\sigma_2 \end{aligned} \tag{28}$$

where $\Delta\sigma_1$ and $\Delta\sigma_2$ denote uncertainties producing by unconsidered target acceleration such as the target acceleration, axis transformation error, etc.. Note that the second sliding manifold σ_2

is redefined with respect to the acceleration implied in a direction of body z-axis and all errors caused by the redefinition is considered in $\Delta\sigma_2$. Similarly, considering uncertainties or parameters which are difficult to measure such as the actuator deflection angular rate η gives the equation of motion rewritten as:

$$\begin{aligned}
\dot{x}_1 &= \frac{x_2}{\rho} + \Delta\sigma_1 \\
\dot{x}_2 &= -\dot{\rho}\dot{\lambda} + x_3 + \Delta\sigma_2 \\
\dot{x}_3 &= \bar{Z}_A x_3 + \bar{Z}_q x_4 + \Delta A_z \\
\dot{x}_4 &= \bar{M}_A x_3 + \bar{M}_q x_4 + \bar{M}_\delta \delta + \Delta q
\end{aligned} \tag{29}$$

where:

$$\begin{aligned}
\mathbf{x} &= [x_1 \;\; x_2 \;\; x_3 \;\; x_4]^T \\
&= [(\lambda - \lambda_c) \;\; V_\lambda \;\; A_z \;\; q]^T
\end{aligned} \tag{30}$$

For the backstepping design, the new residual variables z_1, z_2, z_3 and virtual control states $\mathbf{x}_c$ are proposed as:

$$\begin{aligned}
z_1 &= \lambda - \lambda_c = x_1 \\
z_2 &= V_\lambda - V_{\lambda_c} = x_c - x_{2c} \\
z_3 &= A_z - A_{zc} = x_3 - x_{3c} \\
z_4 &= q - q_c = x_4 - x_{4c}
\end{aligned} \tag{31}$$

Here, the equilibrium point of this system is the origin. Futhermore, the derivatives of the residual variables are obtained by:

$$\begin{aligned}
\dot{z}_1 &= -\dot{\rho}\dot{\lambda} + z_2 + \Delta\sigma_\lambda + x_{2c} \\
\dot{z}_2 &= \bar{Z}_A x_2 + \bar{Z}_q z_3 + \Delta A_z' + \bar{Z}_q x_{3c} - \dot{x}_{2c} \\
\dot{z}_3 &= \bar{M}_A x_2 + \bar{M}_q x_3 + \bar{M}_\delta \delta + \Delta q - \dot{x}_{3c}
\end{aligned} \tag{32}$$

Let us consider the simple Lyapunov function candidate V to analyse the stability of the system:

$$V = \frac{z_1^2}{2} + \frac{z_2^2}{2} + \frac{z_3^2}{2} + \frac{z_4^2}{2} \tag{33}$$

In order to make $\dot{V}$ negative definite, x_{2c}, x_{3c}, x_{4c}, and δ are introduced as:

$$\begin{aligned}
x_{2c} &= \rho\Delta\hat{\sigma}_1 - K_1 z_1 \\
x_{3c} &= \dot{\rho}\dot{\lambda} - \Delta\hat{\sigma}_2 - \frac{z_1}{\rho} - K_2 z_2 \\
x_{4c} &= \frac{1}{\bar{Z}_q}\left[\dot{x}_{3c} - \bar{Z}_A x_3 - \Delta\hat{A}_z - z_2 - K_3 z_3\right] \\
\delta &= \frac{1}{\bar{M}_\delta}\left[\dot{x}_{4c} - \bar{M}_A x_3 - \bar{M}_q x_4 - \Delta\hat{q} - \bar{Z}_q z_3 - K_4 z_4\right]
\end{aligned} \tag{34}$$

where $\Delta\hat{\sigma}_1$, $\Delta\hat{\sigma}_2$, $\Delta\hat{A}_z$, and $\Delta\hat{q}$ are the estimations of $\Delta\sigma_1$, $\Delta\sigma_2$, ΔA_z, and Δq. Substituting equation (34) into the time differentiation of V yields:

$$\begin{aligned}
\dot{V} &= -K_1 z_1^2 - K_2 z_2^2 - K_3 z_3^2 - K_4 z_4^2 \\
&\quad + \Delta\bar{\sigma}_1 z_1 + \Delta\bar{\sigma}_2 z_2 + \Delta\bar{A}_z z_3 + \Delta\bar{q} z_4 \\
&= -a + b
\end{aligned} \tag{35}$$

where:

$$\begin{aligned}
a &= -K_1\left(z_1 - \frac{\Delta\bar{\sigma}_1}{2K_1}\right)^2 - K_2\left(z_2 - \frac{\Delta\bar{\sigma}_2}{2K_2}\right)^2 \\
&\quad - K_3\left(z_3 - \frac{\Delta\bar{A}_z}{2K_3}\right)^2 - K_4\left(z_4 - \frac{\Delta\bar{q}}{2K_4}\right)^2 \\
b &= \frac{\Delta\bar{\sigma}_1^2}{4K_1} + \frac{\Delta\bar{\sigma}_2^2}{4K_2} + \frac{\Delta\bar{A}_z^2}{4K_3} + \frac{\Delta\bar{q}^2}{4K_4^2}
\end{aligned} \tag{36}$$

And:

$$\begin{aligned}
\Delta\bar{\sigma}_1 &= \Delta\sigma_1 - \Delta\hat{\sigma}_1 \\
\Delta\bar{\sigma}_2 &= \Delta\sigma_2 - \Delta\hat{\sigma}_2 \\
\Delta\bar{A}_z &= \Delta A_z - \Delta\hat{A}_z \\
\Delta\bar{q} &= \Delta q - \Delta\hat{q}
\end{aligned} \tag{37}$$

Generally, the first time derivative of Lyapunov function candidate should be negative definite to guarantee stability of the dynamic system for interception. However,for this system, it is possible to prove that this system is always bounded to the convergent sphere, $a = b$, from the condition given by:

$$\begin{cases} \dot{V} \le 0 & \text{for } a \ge b \\ \dot{V} > 0 & \text{for } a < b \end{cases} \tag{38}$$

As shown in equation (35), the performance of integrated guidance and control logic are sensitive to the value of unknown disturbance estimation; $\Delta\hat{\sigma}_1$, $\Delta\hat{\sigma}_2$, $\Delta\hat{A}_z$, and $\Delta\hat{q}$. Well estimated unknown disturbance can help to alleviate the degradation of the tracking performance. Therefore, the disturbance estimator algorithm is introduced in the next section.

5 Sliding Mode Disturbance Observer

As described previous section, the performance of the suggested integrated guidance and control law using backstepping control can be significantly degraded due to the big modelling inaccuracies. In this section, the sliding mode disturbance observer is introduced in order to solve this problem. Consider following first order system dynamic to understand the proposed method that apply robust disturbance observer to the formation guidance law:

$$\begin{aligned} \dot{x}_0 &= f_0(x,u)+d_0 \\ \dot{x} &= f_0(x,u)+d \\ x &= x_0+\xi \end{aligned} \tag{39}$$

where x_0 and x are measurable state without measurement noise and with it, $f_0(x,u)$ is the known function of state and control, and d_0 and d are unknown disturbance term without the noise and with that. In the ref. [8], arbitrary-order exact robust differentiator is introduced and stability and bounndness of the proposed differentiator is proved in the case that $\xi \in [-\varepsilon \ \ \varepsilon]$ is Lebesque-measurable noise. Modification of the robust differentiator is allow to design a sliding mode disturbance observer for estimation of d_0. In this paper, the sliding mode disturbance observer is proposed in the form:

$$\begin{aligned} \dot{s}_0 &= \nu_0 + f_0(x,\ u) \\ \nu_0 &= -\kappa_0|s_0-x|^{n/(n+1)}\mathrm{sign}(s_0-x)+s_1 \\ \dot{s} &= \nu_1 \\ \nu_1 &= -\kappa_1|s_1-\nu_0|^{(n-1)/n}\mathrm{sign}(s_1-\nu_0)+s_2 \\ &\vdots \\ \dot{s}_{n-1} &= \nu_{n-1} \\ \nu_{n-1} &= -\kappa_{n-1}|s_0-x|^{1/2}\mathrm{sign}(s_{n-1}-\nu_{n-2})+s_n \\ \dot{s}_n &= -\kappa_n \mathrm{sign}(z_n-\nu_{n-1}) \end{aligned} \tag{40}$$

As introduced in ref. [8], define functions $\pi_0 = s_0 - x_0(t)$, $\pi_1 = s_1 - d_o(t)$, $\pi_2 = s_2 - \dot{d}_0(t)$, $\cdots$, $\pi_n = s_n - d_0^{(n-1)}$, $\xi = x - x_0$. Then any solution of equation (40) satisfies the differential inclusion understood in the Filippov sense, such that:

$$\begin{aligned} \dot{\pi}_0 &= \nu_0 + f_0(x,u) - f_0(x,u) - d_0 \\ &= -\kappa|\pi_0+\xi(t)|^{n/(n+1)}\mathrm{sign}(\pi_0+\xi(t))+\pi_1 \end{aligned} \tag{41}$$

and:

$$\begin{aligned} \dot{\pi}_1 &= -\kappa_1|\pi_1-\dot{\pi}_0|^{(n-1)/n}\mathrm{sign}(\pi_1-\dot{\pi}_0)+\pi_2 \\ &\vdots \\ \dot{\pi}_{n-1} &= -\kappa_{n-1}|\pi_{n-1}-\dot{\pi}_{n-2}|^{1/2} \\ &\quad \mathrm{sign}(\pi_{n-1}-\dot{\pi}_{n-2})+\pi_n \\ \dot{\pi}_n &\in -\kappa_n \mathrm{sign}(\pi_n-\dot{\pi}_{n-1})+[-L,\ L] \end{aligned} \tag{42}$$

Although the observer is modified from the differentiator in ref.[8], these equations are the same as the differential inclusion in the reference. Therefore, the stability and boundness of the proposed observer can be derived in the exactly same way as the reference's:

Theorem 5.1 *The parameters being properly chosen, the following equalities are true in the absence of input noise after a finite time of a transient process*

$$s_0 = x_0(t); \quad s_i = \nu_{i-1} = d_o^{(i-1)}(t), \quad i = 1,\cdots,n \tag{43}$$

Proof. See the ref. [8].

Theorem 5.2 *Let the input noise satisfy the inequality:*

$$|x(t)-x_0(t)| \le \varepsilon \tag{44}$$

Then the following inequalities are established in finite time for some positive constants μ_i, ς_i depending exclusively on the parameters of the observer:

$$\begin{aligned} |s_0-x_0| &\le \mu_0\varepsilon, \\ |s_i-d_0^{(i-1)}| &\le \mu_i\varepsilon^{(n-i+1)/(n+1)},\ i=1,\cdots,n \\ |\nu_i-d_0^{(i)}| &\le \varsigma_i\varepsilon^{(n-i)/(n+1)},\ i=0,\cdots,n \end{aligned} \tag{45}$$

Table 1 Initial conditions for the simulation

	Missile	Target
position(km, km)	(0, 0)	(4, 1)
Bearing angle(deg)	0	30
Ground speed(m/s)	300	100

Proof. See the ref. [8].

From the theorems, it is clear that s_1 converges to d_0 in a finite time. Moreover, the convergent sphere of the proposed integrated algorithm with the observer in the absence of noises converges into stable point $[0,\ 0,\ 0]^T$.

6 Engagement Simulation

The effectiveness and applicability of the proposed integrated guidance and control logic is verified by numerical simulations. The longitudinal dynamics of the aerial vehicle and dynamics of engagement geometry are used. The missile and target velocity is assumed to be constant and two different evasive manoeuvres of the target, 0g and 1g acceleration, are considered. The initial conditions for the engagement simulation are given in Table 1. And, three desired impact angles, $0(deg)$, $45(deg)$, and $90(deg)$, are considered in the numerical simulation. The aerodynamic characteristics missile is listed as follows:

$$\begin{aligned} Z_\alpha = -0.6,\ \ Z_\delta = -0.116 \\ M_\alpha = -30,\ \ M_q = -1.8,\ \ M_\delta = -80 \end{aligned} \tag{46}$$

It is assumed that the actuator model used for simulation has a first order lag dynamics with the deflection limit $\pm 30deg$:

$$\frac{\delta}{\delta_c} = \frac{100}{s+100} \tag{47}$$

The proposed guidance and control algorithm with the high order disturbance observer is applied in order to validate its performance, and the results are represented in Table 2, Fig. 3, and Fig. 4. The trajectories for each desired impact angle

Table 2 Impact angle

Desired Value	0g Case	1g Case
$0(deg)$	$-0.02(deg)$	$0.92(deg)$
$45(deg)$	$44.79(deg)$	$50.01(deg)$
$90(deg)$	$89.14(deg)$	$95.85(deg)$

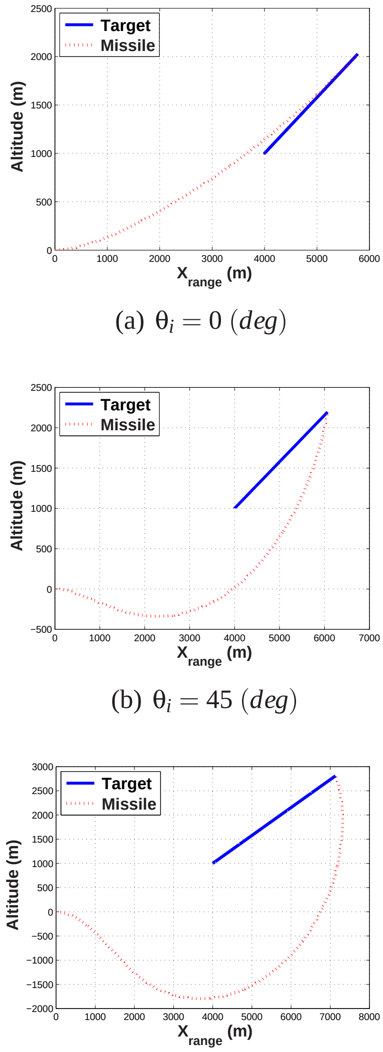

(a) $\theta_i = 0\ (deg)$

(b) $\theta_i = 45\ (deg)$

(c) $\theta_i = 90\ (deg)$

Fig. 3 Trajectories with 0g acceleration of the target

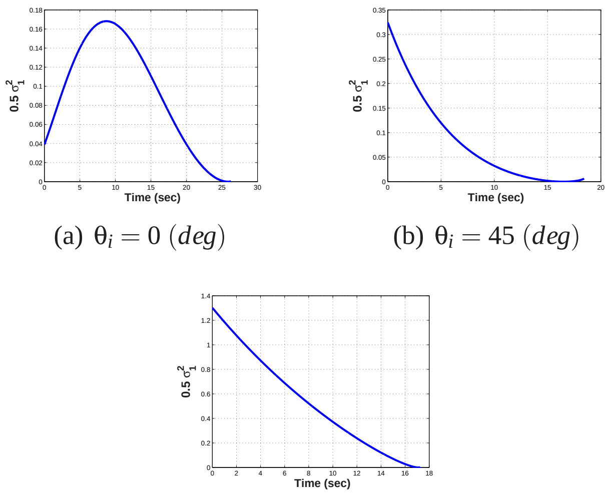

(a) $\theta_i = 0$ (deg) (b) $\theta_i = 45$ (deg)

(c) $\theta_i = 90$ (deg)

Fig. 4 $\frac{1}{2}\sigma_1^2$ with 1g acceleration of the target

is depicted in Fig 3 when there is no target's evasive manoeuvre and real impact angles are represented in the table. As shown in the figure and table, the proposed integrated guidance and control algorithm guarantees that it can intercept the target with the specific terminal angle constraint under certain conditions. Meanwhile, in order to check that it is essential to consider λ_c different from equation (19), the values of $\frac{1}{2}\sigma_1^2$ for each case are represented in Fig. (4). From the figure and Table 2, it is obvious that the integrated guidance and control law can not satisfy the terminal angle constraint although σ_1 converges to zero. Therefore, as mentioned in section 3.2, λ_c should be redefined when there is target's lateral acceleration.

7 Conclusions

In this paper, a integrated guidance and control algorithm with the terminal angle constraint is proposed by using the backstepping control method. And, the high order disturbance observer is introduce not only to enhance the performance of the proposed approach, but also to estimate parameters which are difficult to sensor or have disturbances such as modelling errors. The performance of the proposed algorithm is verified using numerical engagement simulation examples after analysing the stability and robustness of the algorithm using Lyapunov stability theorem. Whilst the proposed method can guarantee the interception satisfying the constraint for the case that there is no acceleration of the target, we have to consider more simulation conditions to check the performance of the method. And, it is necessary to redefine the λ_c for the case that there is target's lateral acceleration.

References

[1] Zarchan, P. *Tactical and strategic missile guidance*, 2nd edition, AIAA tactical missile series., 1994.

[2] Lin, C.-F. *Modern Navigation Guidance and Control Processing*, 2nd Volume, Prentice-Hall, 1991.

[3] Koren, K. and Idan, M. Integrated sliding mode guidance and control for a missile with on-off actuators. *Jounal of Guidanc, Control, and Dynamics*, Vol. 31, No. 4, pp. 204-214, 2008.

[4] Menon, P. K., and Ohlmeyer, E. J. Integrated design of agile missile guidance and autopilot systems. *Control Engineering Practice*, Vol. 9, No. 10, pp. 1095-1106, 2001.

[5] Chwa, D. and Choi, J. Y. Adaptive nonlinear guidance considering control loop dynamics. *IEEE Trans. Aerosp. Electron. Syst.*, Vol. 39, No. 4, pp. 1134-1143, 2003.

[6] Chwa, D., Choi, J. Y., Anavatti, S.G. Observer-based adaptive guidance law considering target uncertainties and control loop dynamics. *IEEE Transactions on Control Systems Technology* Vol. 14, No. 1, pp. 112-123, 2006.

[7] Shima, T. Idan, M., and Golan, O. M. Sliding mode control for integrated missile autopilot-guidance. *Jounal of Guidanc, Control, and Dynamics* Vol. 29, No. 2, pp. 250-260, 2006.

[8] Levant, A. Higher-order sliding modes, differentiation and output-feedback control. *International Journal of Control*, Vol. 76, No. 9/10, pp. 924-941, 2003.

[9] Kim, K.-S. Jung, B. Kim, Y. Practical guidance law controlling impact angle. *Proceedings- Institution of Mecanical Engineers Part G Journal of Aerosapce Engineering* Vol. 221, No. 1, pp. 29-36, 2007.

[10] Ryoo, C. K., Cho, H., and Tahk, M. J. Optimal guidance laws with terminal impact angle constraint. *Journal of Guidance, Control, and Dynamics*, Vol.28, No.4, pp.724-732, 2005.

[11] Lee, J. I., Jeon, I. S., Tahk, M. J. Guidance Law to Control Impact Time and Angle. *IEEE Transactions on Aerospace and Electronic Systems*, Vol.43, No.1, pp.301-310, 2007.

[12] Palumbo, N. F., and Jackson, T. D. Integrated Missile Guidance and Control: A State Dependent Riccati Differential Equation Approach. *Proceeding of the IEEE International Conference on Cntrol Applications*, Vol. 1, 0-7803-5446-X, pp. 179-189, 1999.

[13] Vaddi, S. S., Menon, P. K., and Ohlmeyer, E. J. Numerical SDRE approach for missile integrated guidance-control. *Proceeding of the AIAA Guidance, Navigation and Control Conference and Exhibit*, AIAA 2007-6672, pp. 1-15 2007.

[14] Vaddi, S. S., Menon, P. K., and Ohlmeyer, E. J. Target state estimation for integrated guidance-control of missiles. *Proceeding of the AIAA Guidance, Navigation and Control Conference and Exhibit*, AIAA 2007-6838, pp. 1-22, 2007.

Copyright Statement